SEGMENTED AND "EQUIVALENT" REPRESENTATION OF THE CABLE EQUATION

FRANCESCO ANDRIETTI AND GIOVANNI BERNARDINI
Dipartimento di Fisiologia e Biochimica Generali and Dipartimento di Biologia, Universitá degli Studi di Milano, 20133 Milano, Italy

ABSTRACT The linear cable theory has been applied to a modular structure consisting of n repeating units each composed of two subunits with different values of resistance and capacitance. For n going to infinity, i.e., for infinite cables, we have derived analytically the Laplace transform of the solution by making use of a difference method and we have inverted it by means of a numerical procedure. The results have been compared with those obtained by the direct application of the cable equation to a simplified nonmodular model with "equivalent" electrical parameters. The implication of our work in the analysis of the time and space course of the potential of real fibers has been discussed. In particular, we have shown that the simplified ("equivalent") model is a very good representation of the segmented model for the nodal regions of myelinated fibers in a steady state situation and in every condition for muscle fibers. An approximate solution for the steady potential of myelinated fibers has been derived for both nodal and internodal regions. The applications of our work to other cases dealing with repeating structures, such as earthworm giant fibers, have been discussed and our results have been compared with other attempts to solve similar problems.

INTRODUCTION

The linear cable theory, since its first application to the electrotonic conduction of the axon, has been extended to other situations, such as those dealing with dendrites of complex geometries, spherical cells and branching structures (Jack et al., 1975; Leibovic, 1972). Of particular interest is the generalization of the theory to neural processes of nonconstant width (Strain and Brockman, 1975). Many other works deal with the electrical properties of spherical syncytia (Eisenberg et al., 1979) and with the problem of the radial spread of excitation and electrical properties of the T-system in muscular cells (Adrian et al., 1969; Adrian and Peachey, 1973; Jack et al., 1975; Mathias et al., 1977).

In this paper, we extend the cable theory to a system composed of two different subunits, which can be representative of myelinated axons or muscle fibers, for which a simple cable representation is not an adequate model. A first attempt at studying a more simplified system in a steady state situation can be found in Taylor (1963); a different way of solving a similar problem is given in Brink and Barr (1977).

By making use of the theory of finite difference equations, used in connection with the linear cable equations, we have given an analytical treatment to the general problem.

Apart from the theoretical interest in giving a more realistic picture of the time and space behavior of the potential in structures made of repeating units, some experimental implications of our work will be considered in the discussion.

GLOSSARY

Parameters of the Myelinated Fiber

l_2	(nodal length), $1 \cdot 10^{-4}$ cm (Tasaki, 1955)
d	myelinated internal fiber diameter
D	myelinated external fiber diameter
d'	$(d + D)/2$
$R_{m,1}$	(myelinated sheath resistance), 100,000 Ωcm^2 (Tasaki, 1955)
$R_{m,2}$	(axonal membrane resistance), 20 Ωcm^2 (Tasaki, 1955)
$R_{a,1}$	(intracellular resistivity), $R_{a,2} = 140\ \Omega cm = R_a$ (Schwarz et al., 1979)
$C_{m,1}$	(myelinated sheath capacity), $5 \cdot 10^{-6}$ mF/cm^2 (Tasaki, 1955)
$C_{m,2}$	(axonal membrane capacity), $5 \cdot 10^{-3}$ mF/cm^2 (Tasaki, 1955)
$r_{m,1}$	(myelinated sheath resistivity per unit length fiber), $R_{m,1}/\pi d'$ (Ωcm)
$r_{m,2}$	(axonal membrane resistivity per unit length fiber), $R_{m,2}/\pi d$ (Ωcm)
$r_{a,1}$	(intracellular resistivity per unit length fiber), $r_{a,2} = 4R_a/\pi d^2$ (Ω/cm)
$c_{m,1}$	(myelinated sheath capacity per unit length fiber), $\pi d' C_{m,1}$ (mF/cm)
$c_{m,2}$	(axonal membrane capacity per unit length fiber), $\pi d C_{m,2}$ (mF/cm).

MODEL

We shall discuss a model of a segmented cable composed of n identical units, each made of two subunits with different cable properties and length (Fig. 1). We assume an ohmic core conductance, negligible radial voltage gradients, and no external resistance. The time course of the potential in the jth subunit of the kth unit is represented by the well-known linear partial differential equation (Jack et al.,

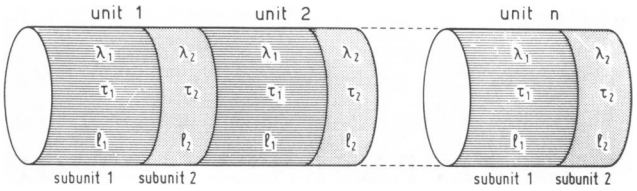

FIGURE 1 Representation of a segmented cable consisting of n units, each one composed of two subunits; λ_1, τ_1, and l_1 are, respectively, the space, the time constant, and the length of subunit 1; λ_2, τ_2, and l_2 are the corresponding parameters of subunit 2.

1975)

$$\lambda_j^2 \frac{\partial^2 V_{k,j}}{\partial x_{k,j}^2} = \tau_{m,j} \frac{\partial V_{k,j}}{\partial t} + V_{k,j}, \tag{1}$$

for $0 \leq x_{k,j} \leq l_j$, where $j = 1$ indicates the first subunit and $j = 2$ indicates the second one. We indicate with l_j the length of the jth subunit, with $r_{m,j}$ the membrane resistance per unit length of the fiber, with $r_{a,j}$ the intracellular resistance to axial flow of current along the fiber, and with $c_{m,j}$ the membrane capacity per unit length of the fiber. $\lambda_j = \sqrt{r_{m,j}/r_{a,j}}$, $\tau_{m,j} = r_{m,j}\, c_{m,j}$ are the jth space and time constants, respectively.

A first set of boundary conditions is due to the continuity of the potential between subunits

$$V_{k,1}(l_1^-, t) = V_{k,2}(0^+, t), \tag{2}$$

$$V_{k,2}(l_2^-, t) = V_{k+1,1}(0^+, t). \tag{3}$$

Taking into account

$$(\partial V_{k,1}/\partial x_{k,1}) = -r_{a,1} I \tag{4}$$

$$(\partial V_{k,2}/\partial x_{k,2}) = -r_{a,2} I, \tag{5}$$

where I is the internal current, function of x and t. For the continuity of I, one has

$$r_{a,2}(\partial V_{k,1}/\partial x_{k,1})_{l_1^-} = r_{a,1}(\partial V_{k,2}/\partial x_{k,2})_{0^+}. \tag{6}$$

Analogously,

$$r_{a,1}(\partial V_{k,2}/\partial x_{k,2})_{l_2^-} = r_{a,2}(\partial V_{k+1,1}/\partial x_{k+1,1})_{0^+}. \tag{7}$$

A way to reduce the segmented model to a uniform one should be that of using the classical cable equations with equivalent parameters (r_m, r_a, c_m) calculated according to the elementary laws of circuitry. One has

$$r_m = [(l_1 + l_2)\, r_{m,1}\, r_{m,2}]/(l_1 r_{m,2} + l_2 r_{m,1}); \tag{8}$$

$$r_a = (l_1 r_{a,1} + l_2 r_{a,2})/(l_1 + l_2); \tag{9}$$

$$c_m = (l_1 c_{m,1} + l_2 c_{m,2})/(l_1 + l_2); \tag{10}$$

and

$$\lambda = \sqrt{r_m/r_a},\ \tau_m = r_m\, c_m.$$

For the equivalent cable, the time course of the potential will be (Jack et al., 1975)

$$V(x, t) = (V_0/2)\,[\exp(-X)\,\mathrm{erfc}(X/2\sqrt{T} - \sqrt{T}) + \exp(X)\,\mathrm{erfc}(X/2\sqrt{T} + \sqrt{T})] \tag{11}$$

for a constant step of potential in $x = 0$ as boundary condition, or

$$V(x, t) = (r_a I_0 \lambda/4)\,[\exp(-X)\,\mathrm{erfc}(X/2\sqrt{T} - \sqrt{T}) - \exp(X)\,\mathrm{erfc}(X/2\sqrt{T} + \sqrt{T})] \tag{12}$$

for a constant current in $x = 0$. Here $X = x/\lambda$, $T = t/\tau_m$, and V_0 and I_0 are the amplitudes of the voltage and the current steps, respectively.

In fact, because of the distributed properties of the parameters along the cable length, the use of the equivalent model does not give the same results of the segmented one, as should be the case for a discrete elements circuit. One of the aims of the present work, which we will develop in the following pages, is to evaluate the error introduced by the use of Eqs. 11 or 12 with respect to the true solutions of the segmented model.

ANALYTICAL METHOD

Taking into account the boundary condition $V(x,0) = 0$, one obtains from Eq. 1:

$$\lambda_j^2 \frac{\partial^2 \bar{V}_{k,j}}{\partial x_{k,j}^2} = \tau_{m,j} \bar{V}_{k,j}\, s + \bar{V}_{k,j}, \tag{13}$$

where $\bar{V}_{k,j}(x, s)$ is the Laplace transform of $V_{k,j}(x, t)$ with respect to t. The general solution of Eq. 13 in the k,j subunit is

$$\bar{V}_{k,j}(x, s) = A_{k,j}(s) \exp[x_{k,j}\, \phi_j(s)/\lambda_j] + B_{k,j}(s) \exp[-x_{k,j}\, \phi_j(s)/\lambda_j], \tag{14}$$

where $\phi_j(s) = \sqrt{\tau_{m,j} s + 1}$ and $A_{k,j}(s)$ and $B_{k,j}(s)$ are functions of s to be determined by means of the boundary conditions. From Eqs. 2 and 14, one has

$$A_{k,1}(s) \exp[l_1 \phi_1(s)/\lambda_1] + B_{k,1}(s) \exp[-l_1 \phi_1(s)/\lambda_1] = A_{k,2}(s) + B_{k,2}(s). \tag{15}$$

Analogously, from Eqs. 3 and 14 one has

$$A_{k,2}(s) \exp[l_2 \phi_2(s)/\lambda_2] + B_{k,2}(s) \exp[-l_2 \phi_2(s)/\lambda_2] = A_{k+1,1}(s) + B_{k+1,1}(s). \tag{16}$$

From Eqs. 6 and 14 one has

$$\frac{r_{a,2}\phi_1(s)}{\lambda_1}\{A_{k,1}(s) \exp[l_1 \phi_1(s)/\lambda_1] - B_{k,1}(s) \exp[-l_1 \phi_1(s)/\lambda_1]\} = \frac{r_{a,1}\phi_2(s)}{\lambda_2}[A_{k,2}(s) - B_{k,2}(s)]. \tag{17}$$

Analogously, from Eqs. 7 and 14,

$$\frac{r_{a,1}\,\phi_2(s)}{\lambda_2}\{A_{k,2}(s)\exp[l_2\phi_2(s)/\lambda_2] - B_{k,2}(s)\exp[-l_2\phi_2(s)/\lambda_2)\}$$

$$= \frac{r_{a,2}\,\phi_1(s)}{\lambda_1}[A_{k+1,1}(s) - B_{k+1,1}(s)]. \quad (18)$$

Let us now introduce the following notations:

$$A_{k,1}(s) = u_k(s); \quad (19)$$

$$B_{k,1}(s) = v_k(s); \quad (20)$$

$$A_{k,2}(s) = h_k(s); \quad (21)$$

$$B_{k,2}(s) = g_k(s). \quad (22)$$

Moreover,

$$D(s) = \exp[l_1\,\phi_1(s)/\lambda_1]; \qquad D'(s) = \exp[-l_1\,\phi_1(s)/\lambda_1];$$

$$G(s) = D(s)r_{a,2}\,\phi_1(s)/\lambda_1; \qquad G'(s) = D'(s)r_{a,2}\,\phi_1(s)/\lambda_1;$$

$$H(s) = r_{a,1}\,\phi_2(s)/\lambda_2; \qquad T(s) = r_{a,2}\,\phi_1/\lambda_1;$$

$$P(s) = \exp[l_2\,\phi_2(s)/\lambda_2]; \qquad P'(s) = \exp[-l_2\,\phi_2(s)/\lambda_2];$$

$$S(s) = H(s)\,P(s); \qquad S'(s) = H(s)\,P'(s).$$

With the above notations Eqs. 15–18 become

$$D(s)\,u_k(s) + D'(s)\,v_k(s) - h_k(s) - g_k(s) = 0; \quad (23)$$

$$-u_{k+1}(s) - v_{k+1}(s) + P(s)h_k(s) + P'(s)g_k(s) = 0; \quad (24)$$

$$G(s)u_k(s) - G'(s)v_k(s) - H(s)h_k(s) + H(s)g_k(s) = 0; \quad (25)$$

$$-T(s)u_{k+1}(s) + T(s)v_{k+1}(s) + S(s)h_k(s) - S'(s)g_k(s) = 0. \quad (26)$$

In the case of cables of finite length, Eqs. 23 and 25 provide $2n$ conditions and Eqs. 24 and 26 provide $2(n-1)$ conditions to determine the $4n$ unknown functions $A_{k,j}(s)$ and $B_{k,j}(s)$. The last two conditions are given by the value of the potential or its derivative at $x_{1,1} = 0$ and at the end of the cable.

Solutions of the $2n$ linear system can be performed by any classical method such as that of pivot. Such methods require much computer time because they have to be repeated for as many values of s as are needed for the accuracy of the inversion procedure. An explicit solution greatly reduces the computation time, but it is cumbersome to calculate when n increases.

The values of $u_k(s)$, $v_k(s)$, $h_k(s)$, and $g_k(s)$, when $n \to \infty$, are given in the Appendix both for a constant step of potential (Eqs. A12, A13, A1, and A2) and a constant step of current (Eqs. A14, A15, A1, and A2). Substituting these values in Eq. 14, by taking into account Eqs. 19–22, we find

$$\bar{V}_{k,1}(x,s) = \bar{V}(0,s)\,\xi_1^{k-1}(s)\{[r(s) - \xi_1(s)]\exp[x_{k,1}\,\phi_1(s)/\lambda_1] + [\xi_1(s) - q(s)]\exp[-x_{k,1}\,\phi_1(s)/\lambda_1]\}/[r(s) - q(s)];$$

$$\bar{V}_{k,2}(x,s) = \bar{V}(0,s)\,[\xi_1^{k-1}(s)\{\eta(s)[r(s) - \xi_1(s)] + \mu(s)[\xi_1(s) - q(s)]\}\exp[x_{k,2}\,\phi_2(s)/\lambda_2] + \{\epsilon(s)[\xi_1(s) - q(s)] + \delta(s)[r(s) - \xi_1(s)]\} \cdot \exp[-x_{k,2}\,\phi_2(s)/\lambda_2]]/[r(s) - q(s)]$$

for a step of potential and a similar expression for a step of current.

In a steady state situation, Eq. 1 becomes

$$\lambda_j^2 \frac{\partial^2 V_{k,j}}{\partial x_{k,j}^2} = V_{k,j}, \quad (1a)$$

and is subject to the same limit conditions of Eqs. 2–5. To solve Eq. 1a, we can repeat the same procedure given above for the transient case, taking $\tau_{m,j} = 0$. In this case, of course, we will find the true solution instead of its Laplace transform. We will find

$$Du_k + D'v_k - h_k - g_k = 0; \quad (23a)$$

$$-u_{k+1} - v_{k+1} + Ph_k + P'g_k = 0; \quad (24a)$$

$$Gu_k - G'v_k - Hh_k + Hg_k = 0; \quad (25a)$$

$$-Tu_{k+1} + Tv_{k+1} + Sh_k - S'g_k = 0; \quad (26a)$$

where D, D', and so on are now constant functions and are determined according to what was already said. For infinite cables, we will use the same method given above for the transient case.

Although the segmented model is, in principle, always preferable to its simplified version, it is important to explore to what extent the results of the two models are different. In the case of small differences, in fact, the equivalent model should be preferred because it is much easier to handle than the segmented one. It admits the explicit solution given by Eqs. 11 and 12 and it can easily be used to fit experimental curves to the theoretical ones to determine the electrical parameters of the fibers. Instead, for the segmented model, we have obtained explicitly only the Laplace transforms of the solutions, which have to be inverted by a numerical procedure, as we will show in the next section.

NUMERICAL METHODS

The inversion of the Laplace transform $\bar{V}(x,s)$ has been performed according to the well-known inversion formula

$$V_{k,j}(x,t) = \frac{\exp(zt)}{2\pi}\int_{-\infty}^{+\infty}\exp(ity)\,\bar{V}_{k,j}(x, z + iy)dy, \quad (27)$$

where $s = z + iy$ and z is any value for which the Laplace transform of $V_{k,j}(x,t)$ exists. By calling $Re[\bar{V}_{k,j}(x, z + iy)]$

and $Im[\bar{V}_{k,j}(x, z + iy)]$ the real and the imaginary parts of $\bar{V}_{k,j}(x, z + iy)$, we found, respectively, an even and an odd function; this is a guarantee that the Fourier transform of $\bar{V}_{k,j}(x, s)$ on the right-hand side of Eq. 27 is a real function. Moreover, one has

$$V_{k,j}(x, t) = 2\left\{\int_{-\infty}^{+\infty} Re\,[\bar{V}_{k,j}(x, z + iy)] \cos(yt)dy + \int_{-\infty}^{+\infty} Im\,[\bar{V}_{k,j}(x, z + iy)] \sin(yt)dy\right\}.$$

The two integrals can be approximated by a discrete Fourier representation. By doing this, we have made use of an FFT (fast Fourier transform) routine in which $Re[\bar{V}_{k,j}(x, z + iy)]$ and $Im[\bar{V}_{k,j}(x, z + iy)]$ were evaluated in 2^N points at a distance Δy, depending on the time course of the phenomenon. We obtained an average accuracy of more than three digits for $N = 8$ and of five digits for $N = 12$. The average time of computation was ~7 and 50 s, respectively, with a FORTRAN double precision routine on a Univac 1100 elaborator.

Particular care was needed in the calculation of the complex root arising in the solution of Eq. A9. In fact, to avoid discontinuities in the evaluation of $\xi_1(s)$, one has to take into account the number of cycles that the argument of the square root describes around the origin of the complex plane.

APPLICATIONS

Voltage and Current Steps

We will apply our model to two particular situations in which the modular cable structure theory could be of relevance, i.e., the myelinated axons and the skeletal muscle fibers.

For myelinated fibers we have considered the internode as the first subunit ($j = 1$) and the node as the second one ($j = 2$). First, we have chosen, as a boundary condition at the beginning of the fiber, a step of potential V_0. The values of $u_k(s)$, $v_k(s)$, $h_k(s)$, and $g_k(s)$ of the segmented model are given by Eqs. A12, A13, A1, and A2 when one takes into account the Laplace transform $\bar{V}(0, s)$ of the potential in $x_{1,1} = 0$. In this case, $\bar{V}(0, s) = V_0/s$. The potential as a function of time, for both models, is shown in Fig. 2 *A*. The values of $V_{k,j}(x, t)/V_0$ of the segmented model, obtained by numerical inversion of Eq. 14 for four different points on the myelinated fiber (continuous line), together with the potential of the equivalent model given by Eq. 11 (dashed lines), evaluated at the same points, are plotted on the ordinate axis. Because of the linear properties of the model, this ratio is independent of V_0. The values of the parameters of the segmented model are calculated according to the Glossary. Those of the equivalent model are calculated according to Eqs. 8–10. In our computation, we have taken $d = 0.7D$ (Tasaki, 1955) to calculate $r_{m,2}$, $r_{a,1}$, $c_{m,2}$, and $r_{a,2}$, and $d' = (d + D)/2 = 0.85D$ to calculate $c_{m,1}$ and $r_{m,1}$ to try

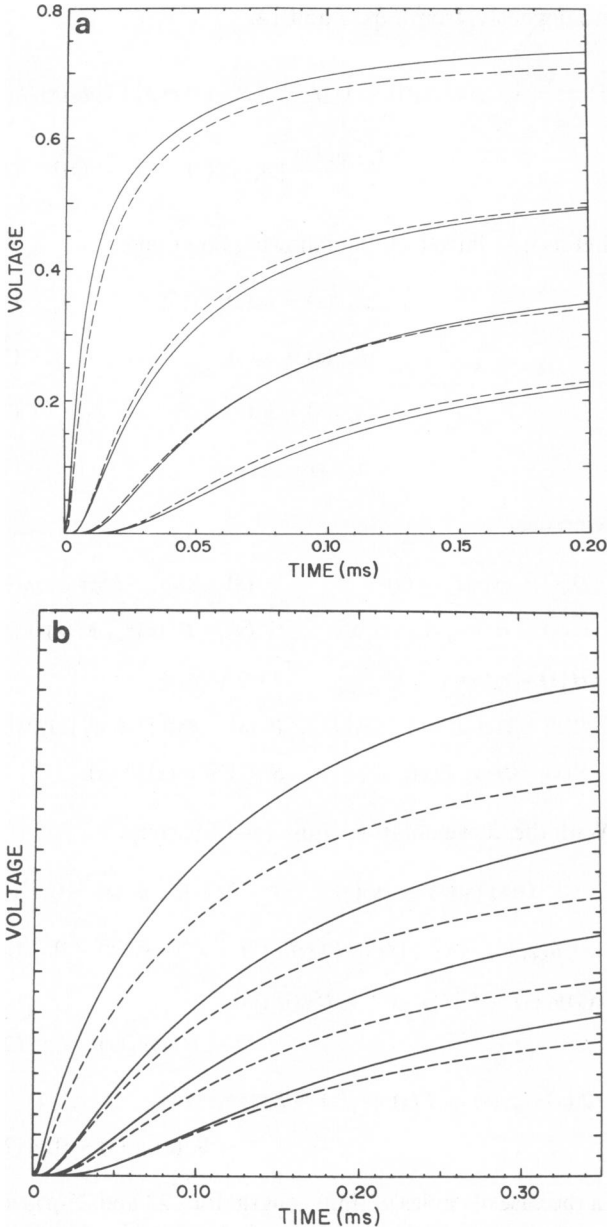

FIGURE 2 Time course of the potential for the segmented (continuous lines) and the equivalent (dashed lines) model at different points along the myelinated fiber; from the top: middle of the first internode, middle of the first node, middle of the second internode, middle of the second node. (*a*) Step of potential; (*b*) step of current.

to take into account the myelin sheath width. The internodal length is calculated according to Hursh (1939) as $l_1 = 100D$. We have taken a value of D of 15 μm which can be considered representative of a class of large motor axons. The asymptotic values of curves of Fig. 2 *A* should be read on the intermediate curve of Fig. 3 *A* in which the steady state values of the potential are plotted as a function of the distance along the myelinated fiber, together with the steady state values of the equivalent cable, for different values of D.

As a second case, we have considered the injection of a

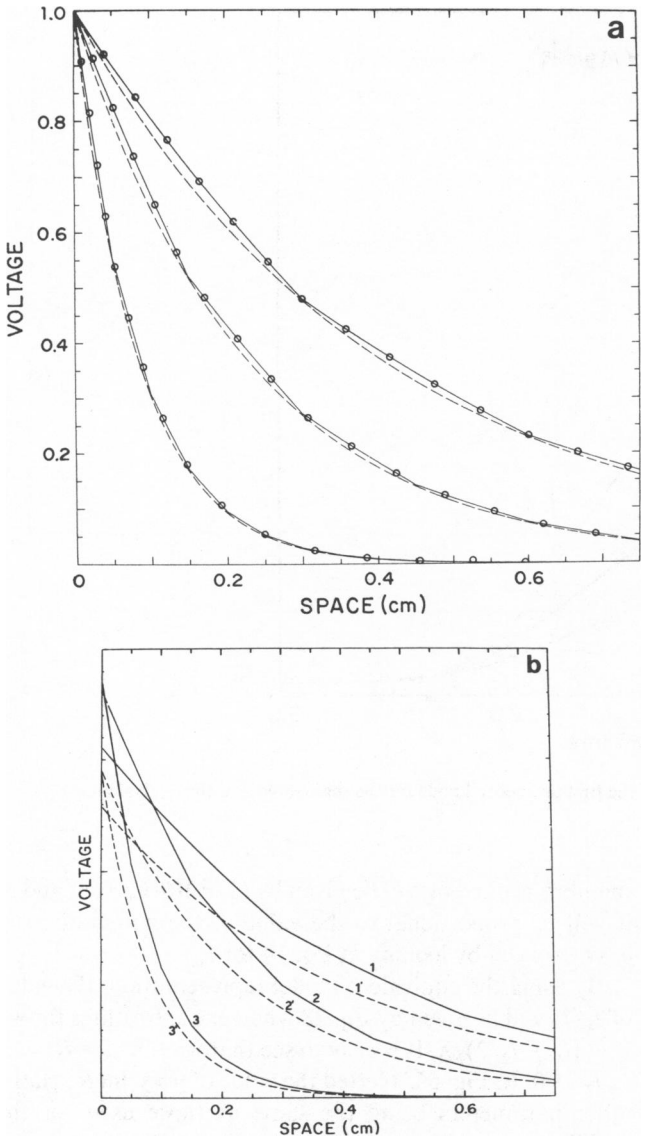

FIGURE 3 Effect of the diameter of the myelinated fiber on the steady state potential for a voltage step (*a*) and for a current step (*b*). (*a*) From the top: D = 30, 15, and 5 μm, segmented (continuous lines) and equivalent (dashed lines) model; the circles represent the approximate solution given by Eqs. 30–31. (*b*) The curves 1, 2, and 3 (continuous lines) correspond to D = 30, 15, and 5 μm for the segmented model; 1′, 2′, and 3′ (dashed lines) are the corresponding curves of the equivalent model. To maintain the values of the ordinates in the same range, the stimulating current has been multiplied for 0.3 for curves 1–1′ and for 2 for 3–3′.

constant step of current I_0 at $x_{1,1} = 0$. Under this condition, the values of $u_k(s)$, $v_k(s)$, $h_k(s)$, and $g_k(s)$ are given by Eqs. A14, A15, A1, and A2, taking into account the fact that

$$\left(\frac{\partial V_{1,1}}{\partial x_{1,1}}\right)_{x_{1,1}=0} = -r_{a,1} I_0/2,$$

so that

$$\bar{V}'(0, s) = -r_{a,1} I_0/2s.$$

The results for both the segmented and the equivalent model evaluated at the same points of Fig. 2 *A* are shown in Fig. 2 *B* for the transient situation and D = 15 μm. Because of the linear properties of the potential with respect to I_0, the values of the ordinate axis are now in arbitrary units. The corresponding steady state situations should be read on the (2–2′) cureves of Fig. 3 *B*.

We see that the discrepancy between the two models decreases along the fiber length. The effect of the diameter of the fiber on the steady potential is represented in Fig. 3 *B*. Note that when normalized to the same potential at x = 0, the curves of Fig. 3 *B* reduce to those of Fig. 3 *A*.

In our analysis of the spread of the electrotonic potential in myelinated axons we did not take into account some recent models that also consider some leakage of current between the axonal and the Schwann cell membrane (Barret and Barret, 1982). Also, if such models may explain the existence of a slow component in the passive electrotonic response, their incorporation in our work would increase the complexity of the mathematical treatment without greatly affecting the results concerning the difference between the segmented and the equivalent model.

Another possible candidate for our analysis is the muscle fiber, considered as a segmented cable in which the two different subunits are the intertubular (j = 1) and the tubular (j = 2) region. There are many ways to represent the effect of the tubular mesh of the T-system (Adrian et al., 1969; Adrian and Peachey, 1973; Jack et al., 1975; Mathias et al., 1977). In any case, a parallel resistance and capacitance pathway may be sufficient to describe the superficial spread of potential (Jack et al., 1975, pp. 105–107). In fact, by the use of a model describing the radial spread of potential in the T-system (Adrian et al., 1969; Mathias et al., 1977), it is possible to obtain values of $R_{m,2}$ and $C_{m,2}$, giving the resistance and capacitance of the T-system per unit area of fiber surface. By using the data of Adrian et al. (1969), we have found that the difference between the equivalent and the segmented model is <1% for a step of current. The reason for this lies in the shortness of the tubular and intertubular regions. In fact, according to Peachey (1965), we have taken $l_1 = 0.25 \times 10^{-3}$ cm and $l_2 = 0.25 \times 10^{-5}$ cm. The results should be different when an access resistance at the opening of the tubular mouth is considered, but this resistance is so low (Adrian and Peachey, 1973) that its possible effect may be neglected with respect to many other possible sources of error as we have checked by numerical computation.

Action Potential Propagation in Narcotized Fibers

An action potential generated at x = 0 spreads electrotonically along the narcotized fiber. In this case $\bar{V}(0, s)$ will be given by the Laplace transform of the action potential calculated by a numerical procedure similar to that seen above. The potential as a function of time is shown in Fig. 4

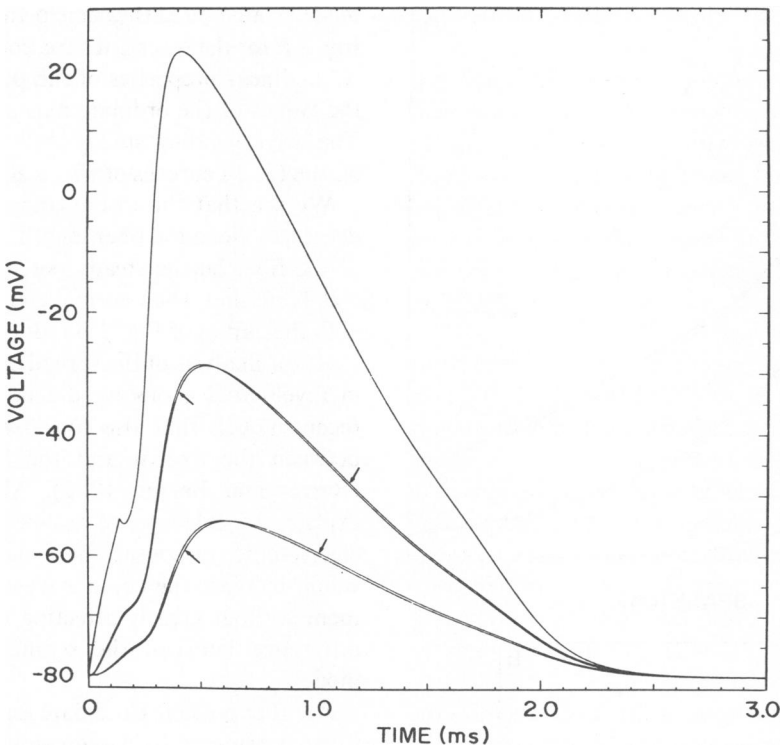

FIGURE 4 Propagated action potential in a narcotized fiber in the middle of the first and second node for the segmented and the equivalent model (arrow). For the values of parameters, see the text.

for both the segmented and the equivalent model at the first and second nodes, for the same parameter values of Fig. 2 *A*. The action potential in $x = 0$ is calculated according to the data of Chiu et al. (1979). We see that the attenuation factor for the potential between two adjacent nodes is ~0.5.

DISCUSSION AND CONCLUSIONS

In conclusion, our analysis shows that the use of the equivalent model approximation may lead to significant errors only in the case of myelinated axons. Moreover, the difference between the two models decreases with the diameter of the fiber, as is shown in Fig. 3. By inspection of Fig. 3 *A*, we see that the agreement is maximal in the nodes, where the two curves are practically indistinguishable.

An early attempt to solve the problem of the passive spread of potential in medullated axons has been given in Taylor (1963), assuming that no sheath leakage is present in the internodal regions. In this case, one finds

$$I_k/I_0 = \exp(-w'k), \tag{28}$$

where I_k is the membrane current in the kth node, I_0 is the membrane current in $x = 0$, and

$$w' = \cosh[1 + 2R_a l_1 l_2/(dR_{m,2})]. \tag{29}$$

Observe that from cable theory (Jack et al., 1975) the membrane current will be given by $(1/r_a)(\partial^2 V/\partial x^2)$, and so it will be proportional to the value of the potential, as is easy to check by looking at Eq. 14 for $\tau_{m,j} = 0$.

By using the equivalent model representation, the value of I_k/I_0 will be given by Eq. 28 when one substitutes for w', $w = (l_1 + l_2/2)/\lambda$. It is easy to see that $w \to w'$ for $R_{m,1} \to \infty$, $l_2 \to 0$. In Fig. 5 is plotted the value of w vs. $\ln(R_{m,1})$, the other parameters being the same as those used for the middle curve of Fig. 3 *A*. For the value of $R_{m,1}$ given in the

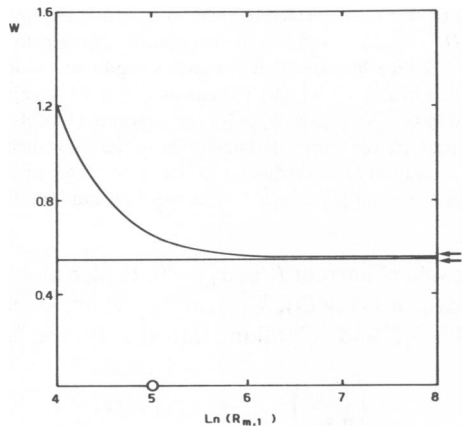

FIGURE 5 Plot of w vs. $\ln(R_{m,1})$, the other parameters being the same as the middle curve of Fig. 3 *a*; the horizontal line corresponds to the constant value of w' for the same set of parameters. The arrows indicate the difference due to the finite value of l_2 (see text).

Glossary (dot), one sees that there is a relevant difference between the two exponents.

To our knowledge, there are no recent published experimental recordings of electrotonic potentials in myelinated fibers to be compared with the calculated results. In an old report of Tasaki and Takeuchi quoted in Cole (1968, p. 378), one finds that the attenuation factor for a propagated action potential in a narcotized fiber ranges between 0.3 and 0.5. We have seen that our results, with the parameter values of Fig. 4, fall in the same range of values.

A particular case of segmented cable is that of the earthworm giant septate fibers (Brink and Barr, 1977). In this case, the nexal resistance is confined to a very short length of fiber, i.e., $l_2 \to 0$. In Fig. 6, we have plotted the steady state potential calculated with the method given in Brink and Barr (1977), together with the corresponding equivalent solutions with equivalent parameters $r_m = r_{m,1}$ and $r_a = r_{a,1} + r_s/l_2$. The values of r_s (nexal resistance), $r_{a,1}$, and $r_{m,1}$, taken from Brink and Barr (1977), are given in the legend of the figure. We see the agreement between the two solutions in the region of septa.

To summarize our results, we want to observe that the use of the equivalent parameters (Eqs. 8–10) is a kind of averaging procedure of the values of two subunits with different properties. Thus, it becomes quite obvious to find the closer agreement between the segmented and the equivalent solutions at both ends of each unit, i.e., at the end of each repeating structure on which the averaging procedure has been performed. This is the reason why the segmented solution matches the equivalent solution at the nodal regions of myelinated fibers and at the nexuses of giant earthworm fibers, as seen in Figs. 3 *A* and 6.

These considerations suggest a way to find an approximate solution of the steady state situation, simply by taking the solutions of the cable equations of the two subunits

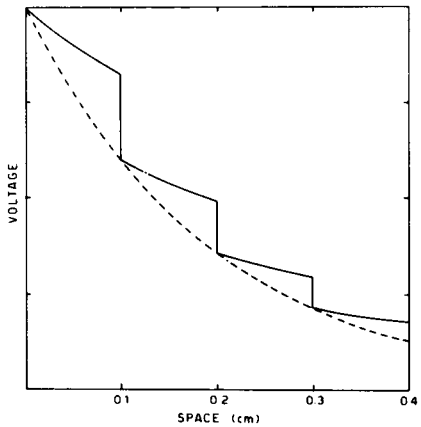

FIGURE 6 Plot of the steady potential of median lateral giant fiber computed through the method given by Brink and Barr (1977) (continuous line) and equivalent representation (dashed line); $r_{m,1} = 300$ KΩcm, $r_{a,1} = 3{,}000$ KΩ/cm, $r_s = 500$ KΩ.

$V_{k,1}(x)$ and $V_{k,2}(x)$ subject to the same end values of the equivalent model and to the conditions of Eqs. 2 and 6. After some calculation, one finds

$$V_{k,1}(x) = A_{k,1} \exp\{[x - (k-1)l]/\lambda_1\} + B_{k,1} \exp\{-[x - (k-1)l]/\lambda_1\} \quad (30)$$

for $(k-1)\,l < x < (k-1)\,l + l_1$, and

$$V_{k,2}(x) = A_{k,2} \exp\{[x - (k-1)\,l - l_1]/\lambda_2\} + B_{k,2} \exp\{-[x - (k-1)\,l - l_1]/\lambda_2\} \quad (31)$$

for $(k-1)l + l_1 < x < kl$, where $l = l_1 + l_2$, and

$$B_{k,1} = \{\exp(l_2/\lambda_2)\, V_k^0 [\exp(l_1/\lambda_1) Q_2 S_2 C_1 + \exp(l_1/\lambda_1) Q_1 S_1 C_2 - Q_2 S_2] - V_k'(Q_1 S_1 C_2 + Q_1 S_1 S_2)\}/[2 \exp(l_2/\lambda_2) \cdot S_1 (Q_2 S_2 C_1 + Q_1 S_1 C_2)];$$

$$A_{k,1} = V_k^0 - B_{k,1};$$

$$A_{k,2} = -\{V_0^k Q_2 + V_k'[Q_2 C_1 \exp(-l_2/\lambda_2) - Q_1 S_1 \exp(-l_2/\lambda_2) + 2Q_1 C_2 S_1 + 2Q_2 S_2 C_1]\}/[2\exp(l_2/\lambda_2) \cdot (Q_2 S_2 C_1 + Q_1 S_1 C_2)];$$

$$B_{k,2} = [V_k^0 Q_2 \exp(l_2/\lambda_2) - V_k'(Q_2 C_1 - Q_1 S_1)]/ \cdot [2(Q_2 S_2 C_1 + Q_1 S_1 C_2)],$$

where

$$V_k^0 = \exp[-(k-1)\,l/\lambda];$$

$$V_k' = \exp\{-[(k-1)\,l + l_2]/\lambda\};$$

$$S_1 = \sinh(l_1/\lambda_1);$$

$$S_2 = \sinh(l_2/\lambda_2);$$

$$C_1 = \cosh(l_1/\lambda_1);$$

$$C_2 = \cosh(l_2/\lambda_2);$$

$$Q_1 = \sqrt{r_{m,1}\, r_{a,1}};$$

$$Q_2 = \sqrt{r_{m,2}\, r_{a,2}}.$$

In the range of values considered in the present paper, the plot of this equation is not distinguishable from that obtained from the segmented cable analysis, as can be seen in Fig. 3 *A* (circles).

The results are different for the transient case, for which a sensible difference between the segmented and the equivalent model also exists in the nodal regions, as can be seen from Figs. 2 and 4. Instead, when the subunit length becomes very short, as for muscle fibers, the two representations match together on the whole cable length. In this case, the "apparent" resistance and capacity given by Eqs. 8–10, as can be determined, for example, from voltage clamp experiments, can be used without introducing signif-

icant errors in the analysis of the superficial spread of potential in muscular fibers. A consequence of this fact will be considered in the following paper (Andrietti et al., 1984).

Some implications of our work may have an experimental relevance in a re-evaluation of the classical method to estimate the fiber parameters by fitting experimental traces of recorded potentials to the cable equation. The early attempts of Lorente de Nó (quoted in Taylor, 1963) used the approximation of infinite myelin sheath resistance, which we have shown to give consistent overevaluations of the space constant $1/w$. On the contrary, the use of the equivalent cable, which is, moreover, much easier to treat, proves to be a very good approximation of the original segmented model in the nodal regions.

Finally, we want to remark that our analyses regard the spread of excitation in infinite cables. As we have said above, the analysis of finite segmented cables is not very practicable for the transient situation except for very low values of n. Instead, for the steady state case, by using a numerical method to solve Eqs. 23a–26a, we have obtained for the finite cable results similar to those of the infinite case, namely that the difference between the (finite) segmented and the (finite) equivalent model may be relevant for myelinated fibers, but not for muscular ones.

APPENDIX

For cables of infinite length, a solution to Eqs. 23–26 can be found by making use of the theory of difference equations. To do this, we first reduce Eqs. 23–26 to two linear, simultaneous difference equations of the second order. From Eqs. 23 and 25, one obtains

$$h_k(s) = \eta(s)u_k(s) + \mu(s)v_k(s); \tag{A1}$$

$$g_k(s) = \epsilon(s)v_k(s) + \delta(s)u_k(s), \tag{A2}$$

where

$$\eta(s) = [H(s)\,D(s) + G(s)]/2H(s);$$
$$\mu(s) = [H(s)\,D'(s) - G'(s)]/2H(s);$$
$$\epsilon(s) = [G'(s) + H(s)D'(s)]/2H(s);$$
$$\delta(s) = [H(s)\,D(s) - G(s)]/2H(s).$$

By substituting Eqs. A1 and A2 into Eqs. 24 and 26, one has

$$-Eu_k(s) + q(s)u_k(s) - Ev_k(s) + r(s)v_k(s) = 0; \tag{A3}$$

$$-T(s)Eu_k(s) + w(s)u_k(s) + T(s)Ev_k(s) + t(s)v_k(s) = 0, \tag{A4}$$

where $Eu_k(s) = u_{k+1}(s)$ is the displacement operator, and

$$q(s) = P(s)\,\eta(s) + P'(s)\,\delta(s);$$
$$r(s) = P(s)\,\mu(s) + P'(s)\,\epsilon(s);$$
$$w(s) = S(s)\,\eta(s) - S'(s)\,\delta(s);$$
$$t(s) = S(s)\,\mu(s) - S'(s)\,\epsilon(s).$$

Letting

$$M_1(E) = -E + q(s);$$
$$M_2(E) = -T(s)E + w(s);$$
$$N_1(E) = -E + r(s);$$
$$N_2(E) = T(s)E + t(s),$$

Eqs. A3 and A4 become

$$M_1(E)u_k(s) + N_1(E)v_k(s) = 0; \tag{A5}$$

$$M_2(E)u_k(s) + N_2(E)v_k(s) = 0. \tag{A6}$$

By executing the operations $M_2(E)$ on both members of Eq. A5 and $M_1(E)$ on both members of Eq. A6, and by recalling that $EEu_k(s) = Eu_{k+1}(s) = u_{k+2}(s)$, one has, after simplication

$$v_{k+2}(s) + b(s)v_{k+1}(s) + v_k(s) = 0, \tag{A7}$$

where

$$b(s) = -[r(s)T(s) + w(s) - t(s) + q(s)T(s)]/2T(s).$$

The general solution of Eq. A7 is (Jordan, 1950, p. 574)

$$v_k(s) = A(s)\,\xi_1^k(s) + B(s)\,\xi_2^k(s), \tag{A8}$$

where $\xi_1(s)$ and $\xi_2(s)$ are the roots of the equation

$$\xi^2(s) + b(s)\xi(s) + 1 = 0, \tag{A9}$$

and $A(s)$ and $B(s)$ are arbitrary constants (with respect to the index k) to be determined by the limit conditions of the problem. Observe that from Eq. A9 one has $|\xi_1(s)||\xi_2(s)| = 1$, so that, as long as the roots are distinct, one of them, say $\xi_1(s)$, will have an absolute value lower than 1, while $|\xi_2(s)| > 1$. Taking into account the boundary condition of infinite cables, i.e., that the potential and its Laplace transform must vanish at the end of the cable when $k \to \infty$, we have from Eq. 14

$$\lim_{k\to\infty} \{u_k(s) \exp [x_{k,1}\,\phi_1(s)/\lambda_1] + v_k(s) \exp [-x_{k,1}\,\phi_1(s)/\lambda_1]\} = 0$$

and for the arbitrariness of $x_{k,1}$ in the interval $0 \leq x_{k,1} \leq l_1$

$$\lim_{k\to\infty} u_k(s) = 0, \qquad \lim_{k\to\infty} v_k(s) = 0.$$

This means that $B(s) = 0$, otherwise $v_k(s)$ will be unbounded for $k \to \infty$, as $|\xi_2(s)| > 1$. So it will be

$$v_k(s) = A(s)\xi_1^k(s). \tag{A10}$$

From Eq. A5 one has (Jordan, 1950, p. 603)

$$u_k(s) = -A(s)\,\frac{N_1[\xi_1(s)]}{M_1[\xi_1(s)]}\,\xi_1^k(s) = -\frac{-\xi_1(s) + r(s)}{-\xi_1(s) + q(s)}\,A(s)\,\xi_1^k(s). \tag{A11}$$

Determination of $A(s)$ depends on the knowledge of the boundary condition in $x_{1,1} = 0$. When the value of the potential is given in $x_{1,1} = 0$, one finds from Eqs. 14, A10, and A11

$$u_k(s) = \bar{V}(0,s)\,\xi_1^{k-1}(s)\,[r(s) - \xi_1(s)]/[r(s) - q(s)]; \tag{A12}$$

$$v_k(s) = \bar{V}(0,s)\,\xi_1^{k-1}(s)\,[\xi_1(s) - q(s)]/[r(s) - q(s)], \tag{A13}$$

where $\overline{V}(0, s)$ is the Laplace transform of the potential in $x_{1,1} = 0$. The values of $h_k(s)$, $g_k(s)$ are given by Eqs. A1, A2, A12, and A13.

When the derivative of the potential is given in $x_{1,1} = 0$, one obtains from Eqs. 14, A10, and A11

$$u_k(s) = \lambda_1 \overline{V}'(0, s)\, \xi_1^{k-1}(s)\, [r(s) - \xi_1(s)]/ \{\phi_1(s)[r(s) + q(s) - 2\,\xi_1(s)]\}; \quad \text{(A14)}$$

$$v_k(s) = \lambda_1 \overline{V}'(0, s)\, \xi_1^{k-1}(s)\, [\xi_1(s) - q(s)]/ \{\phi_1(s)[r(s) + q(s) - 2\,\xi_1(s)]\}, \quad \text{(A15)}$$

where $\overline{V}'(0, s)$ is the Laplace transform of the derivative of the potential in $x_{1,1} = 0$.

The values of $h_k(s)$, $g_k(s)$ are given by Eqs. A1, A2, A14, and A15. We see that in any case the functions $u_k(s)$, $v_k(s)$, $h_k(s)$, and $g_k(s)$ vanish for $k \to \infty$.

Received for publication 17 May 1983 and in final form 26 January 1984.

REFERENCES

Adrian, R. H., W. K. Chandler, and A. L. Hodgkin. 1969. The kinetics of mechanical activation in frog muscle. *J. Physiol.* (*Lond.*). 204:207–230.

Adrian, R. H., and L. D. Peachey. 1973. Reconstruction of the action potential of frog sartorius muscle. *J. Physiol.* (*Lond.*). 235:103–131.

Andrietti, F., A. Peres, and G. Bernardini. 1984. Analysis of lumped and distributed elements models of cut muscle fibers in Vaseline or sucrose gap preparations. *Biophys. J.* 46:625–630.

Barret, E. F., and J. N. Barret. 1982. Intracellular recording from vertebrate myelinated axons: mechanism of the depolarizing after potential. *J. Physiol.* (*Lond.*). 323:117–144.

Brink, P., and L. Barr. 1977. The resistance of the septum of the median giant axon of the earthworm. *J. Gen. Physiol.* 69:517–536.

Chiu, S. Y., J. M. Ritchie, R. B. Rogart, and D. Stagg. 1979. A quantitative description of membrane currents of rabbit myelinated fiber. *J. Physiol.* (*Lond.*). 292:149–166.

Cole, K. S. 1968. Membranes, Ions, and Impulses. University of California Press. Berkeley, CA. 569 pp.

Eisenberg, R. S., V. Barcilon, and R. T. Mathias. 1979. Electrical properties of spherical syncytia. *Biophys. J.* 25:151–180.

Hursh, J. B. 1939. Conduction velocity and diameter of nerve fibers. *Am. J. Physiol.* 127:131–139.

Jack, J. J. B., D. Noble, and R. W. Tsien. 1975. Electrical Current Flows in Excitable Cells. Clarendon Press, Oxford. 502 pp.

Jordan, C. 1950. Calculus of Finite Differences. Chelsea Publishing Company, New York. 652 pp.

Leibovic, K. N. 1972. Nervous System Theory. Academic Press, Inc., New York. 294 pp.

Mathias, R. T., R. S. Eisenberg, and R. Valdisera. 1977. Electrical properties of frog skeletal muscle fibers interpreted with a mesh model of the tubular system. *Biophys. J.* 17:57–93.

Peachey, L. D. 1965. The sarcoplasmic reticulum and transverse tubules of the frog's sartorius. *J. Cell Biol.* 25:209–231.

Schwarz, W., B. Neumcke, and R. Stampfli. 1979. Longitudinal resistance of axoplasm in myelinated nerve fibers of the frog. *Pfluegers Arch. Eur. J. Physiol.* 379:R41.

Strain, G. M., and W. H. Brockman. 1975. A modified cable model for neuron processes with nonconstant diameters. *J. Theor. Biol.* 51:475–494.

Tasaki, I. 1955. New measurements of the capacity and the resistance of the myelin sheath and the nodal membrane of the isolated frog nerve fiber. *Am. J. Physiol.* 181:639–650.

Taylor, R. E. 1963. Cable theory. *In* Physical Techniques in Biological Research. W. L. Nastuck, editor. Academic Press, Inc., New York. 6:219–262.